XIX. Research and Advanced Concepts

PROPULSION DIVISION

A. Ion Thruster Electron Baffle Sizing, *E. V. Pawlik*

1. Introduction

A 20-cm-diameter electron-bombardment ion thruster of the type described in a JPL Technical Memorandum[1] is currently in use in the solar-electric propulsion system studies under way at JPL (Ref. 1). This thruster employs a two-grid ion accelerating geometry because of the proven reliability of this grid type and consequently does not readily obtain the low level of arc chamber losses that have been obtained by other researchers using a coated single grid (Refs. 2 and 3). In a continuing product improvement effort some optimization of the present design was attempted in order to reduce arc chamber losses. The effect of one component, the electron baffle, was studied and modifications in its geometry were found to present some performance gains.

2. Apparatus

A sketch of the ion thruster used in the program is shown in Fig. 1. The nominal operating range for this thruster is 1000 to 2000 W (0.5 to 1.0-A ion beam current at a net accelerating voltage of 2000 V) of throttleable output beam power at a constant specific impulse near 4000 s. Details of thruster geometry and performance can be found in Footnote 1. The thruster is operated in a 3×7-ft vacuum tank while maintaining pressures on the order of 2×10^{-6} to 8×10^{-6} torr.

The hollow cathode and the mounting arrangement within the pole piece are shown in Fig. 2. The hollow cathode is essentially a plasma device which is supplied gaseous mercury propellant from a vaporizer. It consists of a hollow tube with a 0.100-cm-diameter orifice at the end. The discharge is initiated and maintained by a keeper electrode.

An electron baffle is placed between the cathode and anode to provide a distributed source of electrons to the arc chamber. This electron baffle approach is the same as was first used in Ref. 4 and is necessary in order to minimize arc chamber power losses. The baffle also serves to distribute the mercury propellant flow from the cathode into the arc chamber, directing it radially outward from the cathode pole piece region. This radial flow direction increases the residence time of the mercury atoms within the arc chamber, consequently increasing their probability of ionization.

Four electron baffle sizes were investigated. As the different diameters were tested, the distance between the pole piece and the baffle was varied so as to maintain a constant open area of 7.2 cm^2.

[1]Pawlik, E. V., *Performance of a 20-cm-Diameter Electron-Bombardment Hollow-Cathode Ion Thruster*, Technical Memorandum 33-468. Jet Propulsion Laboratory, Pasadena, Calif. (to be published).

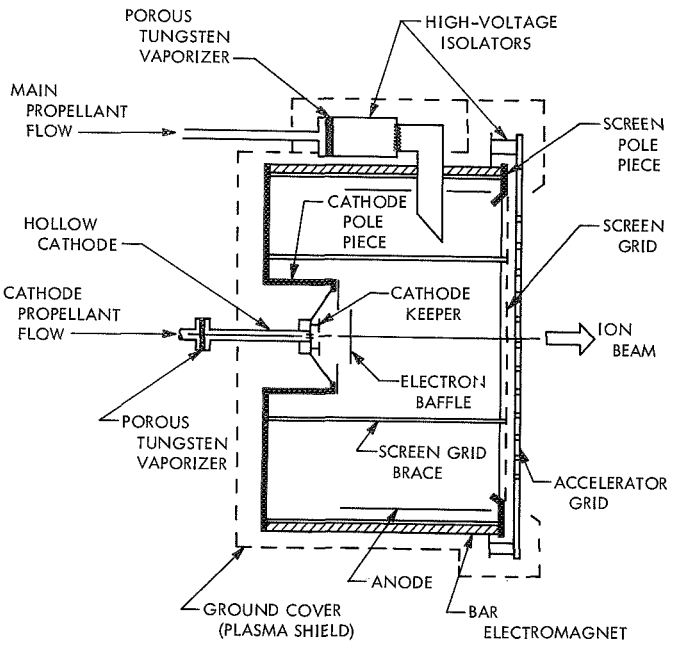

Fig. 1. Sketch of 20-cm-diameter electron-bombardment ion thruster

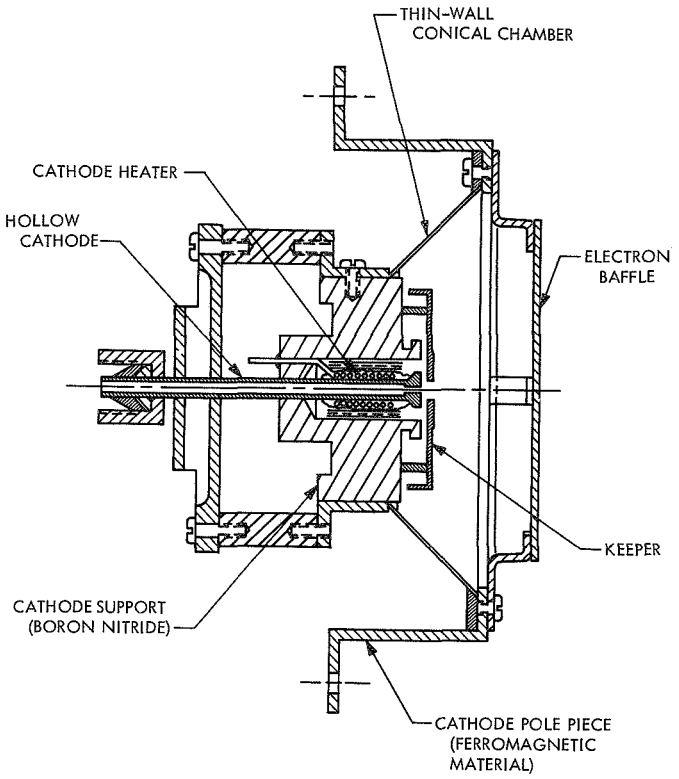

Fig. 2. Cathode pole piece details

The cathode mounting was designed to minimize heat conduction to the thruster. This was accomplished by using a cone of thin stainless steel to support the boron nitride in which the cathode was held.

3. Results and Discussion

Arc chamber losses were measured as the thruster was operated at both the high and low levels of the nominal output power range. These losses, for a propellant utilization near 90% and an arc voltage of 35 V, are plotted in Fig. 3a. For the largest baffle tested the arc was prone to extinguishing at low output power levels. Increasing the current drawn to the keeper electrode from the nominal 0.5 to 1.0 A reduced this tendency somewhat. As the baffle diameter was reduced, the arc chamber losses were reduced, minimizing near a diameter of 4.5 cm for low-power output operation. At high thruster output power, operation with smaller baffles produced lowest arc chamber losses as the diameter was reduced but this was accompanied by extremely noisy arc chamber operation for the two smallest baffle sizes. The cause of this noise is not understood at present. The cathode flow necessary to maintain the arc chamber conditions is shown in Fig. 3b and was found to decrease with baffle diameter. It is believed that the arc voltage could be maintained with less flow as the baffle was reduced because the open area was removed further from the magnetic field at the end of the pole piece, which served as a magnetic restriction to the electron flow in a manner similar to that reported in Ref. 5. The lower cathode flow results in increased main vaporizer flow, creating a more favorable flow distribution and reduced arc chamber losses.

A baffle near 4.7 cm in diameter appears to be an optimum size inasmuch as arc chamber noise problems are avoided. The arc chamber losses are nearly constant with output power for this baffle size and therefore the penalties in throttling thruster output power over the 2:1 range of interest are minimized. Arc chamber losses for this geometry are essentially the same as reported for the thrusters using the single-coated grid.

The keeper voltage as a function of arc current is plotted in Fig. 4 for each of the four baffle sizes investigated. The voltage decreased with increasing current as would be expected for increasing plasma density. The voltage level was lower than that observed for similar hollow-cathode thrusters (Ref. 6). Because of this lower keeper voltage, it is expected that the plasma potential and subsequent cathode orifice wear should be considerably reduced at these levels. Future studies will include measurements of the rate of cathode erosion.

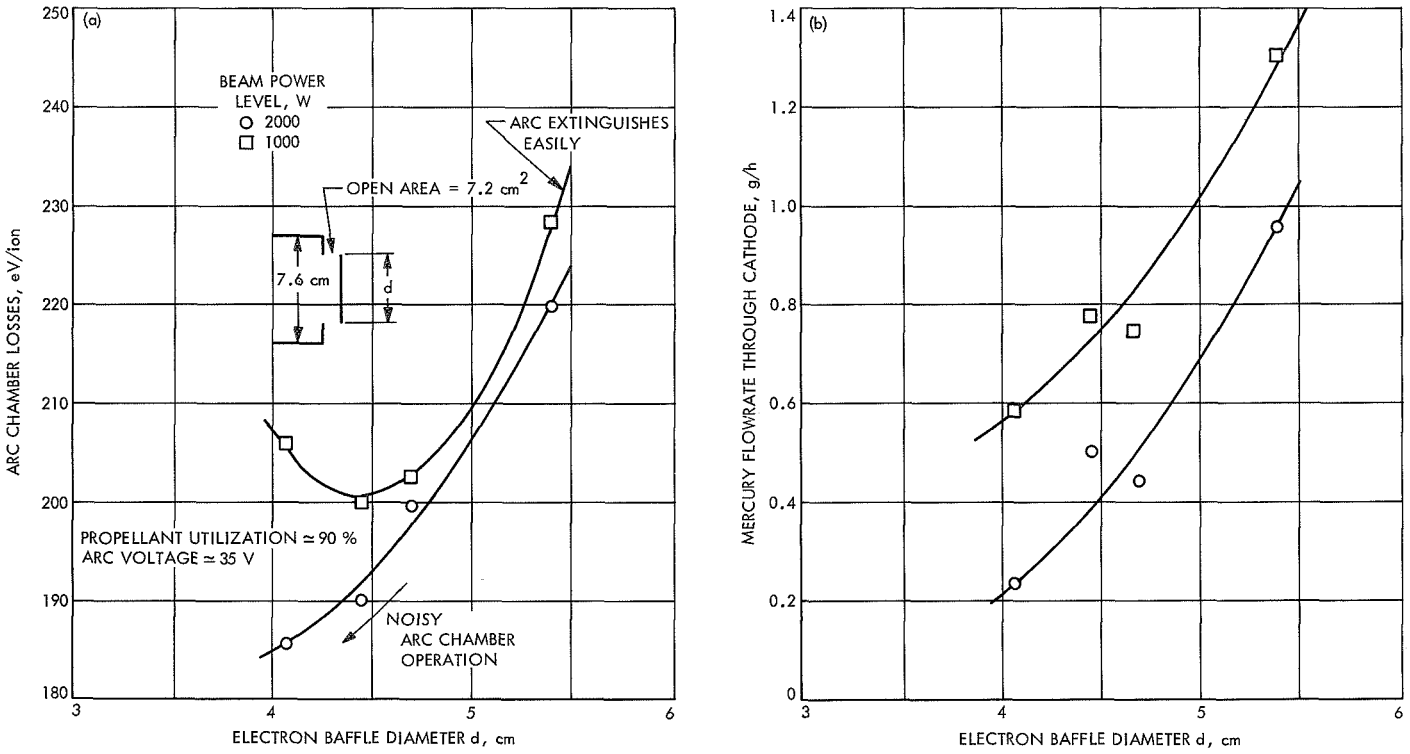

Fig. 3. Effects of electron baffle diameter on (a) arc chamber losses, (b) cathode flow

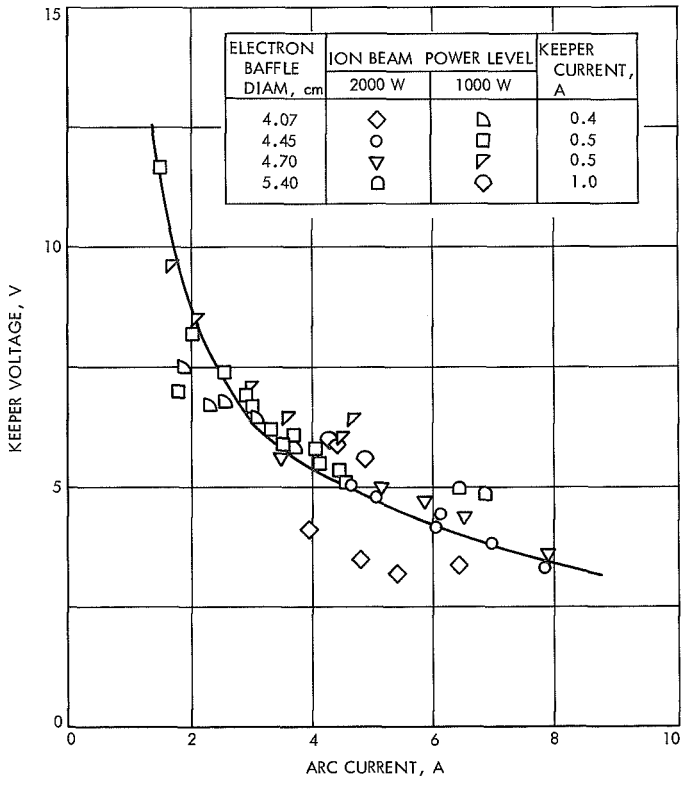

Fig. 4. Effect of arc current on keeper voltage

References

1. Masek, T. D., "Solar Electric Propulsion System Technology," AIAA Paper 70-1153, presented at the 8th Electric Propulsion Conference, Stanford, Calif., Aug. 1970.

2. King, H. J., and Poeschel, R. L., *Low Specific Impulse Ion Engine,* Final Report, NASA CR-72677. Hughes Research Laboratories, Malibu, Calif., Feb. 1970.

3. Bechtel, R. T., "Performance and Control of a 30-Centimeter Diameter Low Impulse Kaufman Thruster," AIAA Paper 69-238, presented at the 7th Electric Propulsion Conference, Williamsburg, Va., Mar. 1969.

4. Eckhardt, W. O., et al., *4,000-hour Life Test of a Liquid-Mercury Cathode in a 20-cm LeRC Ion Thrustor,* special report prepared for NASA (Contract NAS 3-6262). Hughes Research Laboratories, Oct. 1966.

5. Poeschel, R. L., and Knauer, W., "A Variable Magnetic Baffle for Hollow Cathode Thrusters," AIAA Paper 70-175, presented at the 8th Aerospace Sciences Meeting, New York, N.Y., Jan. 1970.

6. Bechtel, R. T., "Component Testing of a 30-Centimeter Diameter Electron Bombardment Thruster," AIAA Paper 70-1100, presented at the 8th Electric Propulsion Conference, Stanford, Calif., Aug. 1970.

B. An Ion Thruster Utilizing a Combination Keeper Electrode and Electron Baffle,

E. V. Pawlik

1. Introduction

Intense interest has recently been focused on using solar-electric-powered spacecraft for deep space missions. Experimental systems work is therefore being conducted (Ref. 1)[1] at JPL using an ion thruster with a hollow-cathode electron source and employing mercury as the propellant. Some thruster improvements, such as a reduction of both cathode operating temperature and arc chamber losses, have been described in SPS 37-64, Vol. III, pp. 146–149, and in the preceding article, *Section A*. A portion of the present systems work has been directed toward experimentally examining the effects on thruster operation of eliminating the chamber in which the cathode is customarily mounted (Refs. 2 and 3). This is of interest since the ions generated within this region are trapped within it and contribute mainly to thruster losses (Ref. 4).

2. Test Setup

A sketch of the 20-cm-diameter ion thruster used in the program is shown in Fig. 1. The nominal operating level for this thruster is 1000 to 2000 W (0.5 to 1.0-A ion beam current at 2000 V) of throttleable output beam power at a constant specific impulse near 4000 s. Details of thruster performance can be found in Footnote 1. The thruster is operated in a 3×7-ft vacuum tank while maintaining pressures on the order of 2×10^{-6} to 8×10^{-6} torr.

Two ways of mounting the hollow cathode within the thruster are shown in Fig. 2. Case I contains the conventional cathode ion chamber and Case II employs a combination keeper electrode and electron baffle. The keeper is necessary to initiate and maintain the cathode discharge. The electron baffle serves to distribute electrons into the arc chamber plasma in a manner so as to minimize arc

[1]Also Pawlik, E. V., *Performance of a 20-cm-Diameter Electron-Bombardment Hollow-Cathode Ion Thruster*, Technical Memorandum 33-468. Jet Propulsion Laboratory, Pasadena, Calif. (to be published).

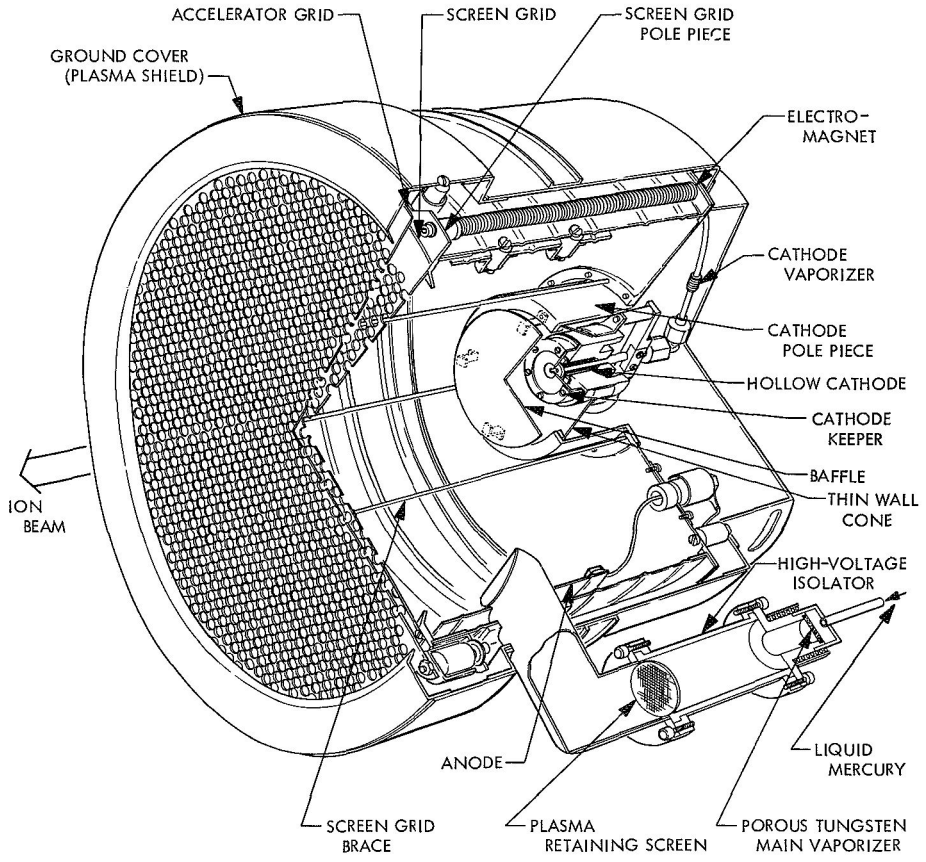

Fig. 1. 20-cm diameter electron-bombardment ion thruster

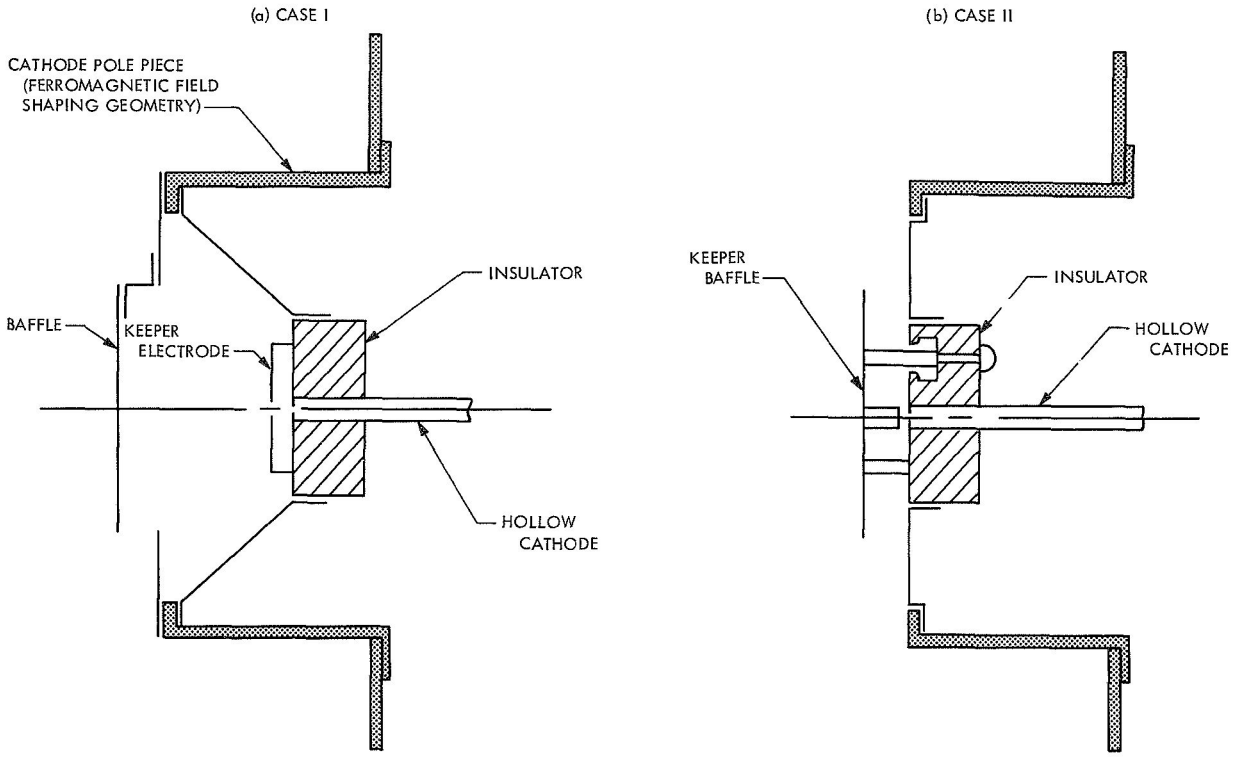

Fig. 2. Cathode mounting details: (a) Case I, cathode mounted within pole piece; (b) Case II, cathode mounted at end of pole piece and using a combination keeper electrode and electron baffle

chamber losses. These two items have been combined into a single unit. The cathode orifice (1.0-mm diam) and electron baffle (4.7-cm diam) used were the optimum sizes as determined in SPS 37-64, Vol. III, and the preceding article, *Section A*.

3. Test Results

The thruster was operated at both the high and low regions of the normal operating range. The discharge chamber loss (the most significant thruster loss) is shown plotted against propellant utilization in Fig. 3. Two values of current to the keeper electrode were examined. Thruster operation was well behaved and insensitive to keeper current levels over the majority of the thruster operating range that was investigated. Some high amplitude oscillations of the arc current were found at low propellant utilizations when operating at low beam power. This instability is well outside of the nominal 90% propellant utilization operating region. The arc chamber losses were essentially the same as those obtained for this configuration shown as Case I in Fig. 2 (reference preceding article, *Section A*). This suggests that significant losses still exist within the cathode-to-keeper region or that there are additional arc chamber losses by electrons being attracted to the ion chamber side of the baffle. The fact that these

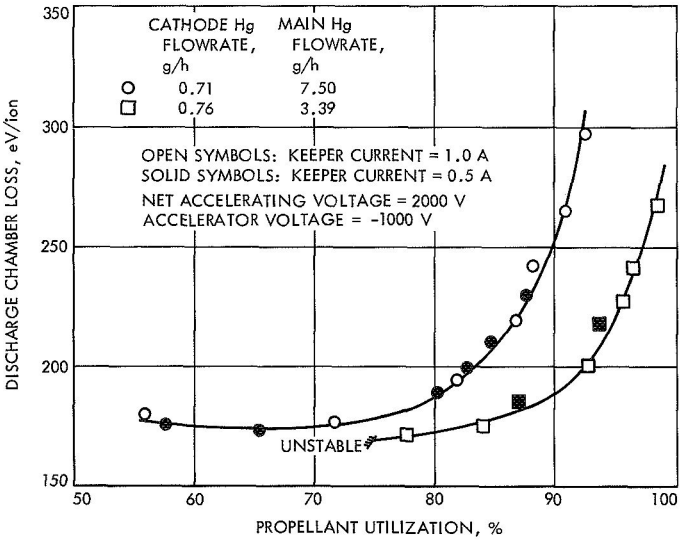

Fig. 3. Thruster arc chamber performance

losses do not change with keeper current levels indicates that electrons withdrawn from the arc chamber are not, however, a major loss mechanism.

An advantage that was found in using the combined keeper–baffle geometry was the elimination of arc current

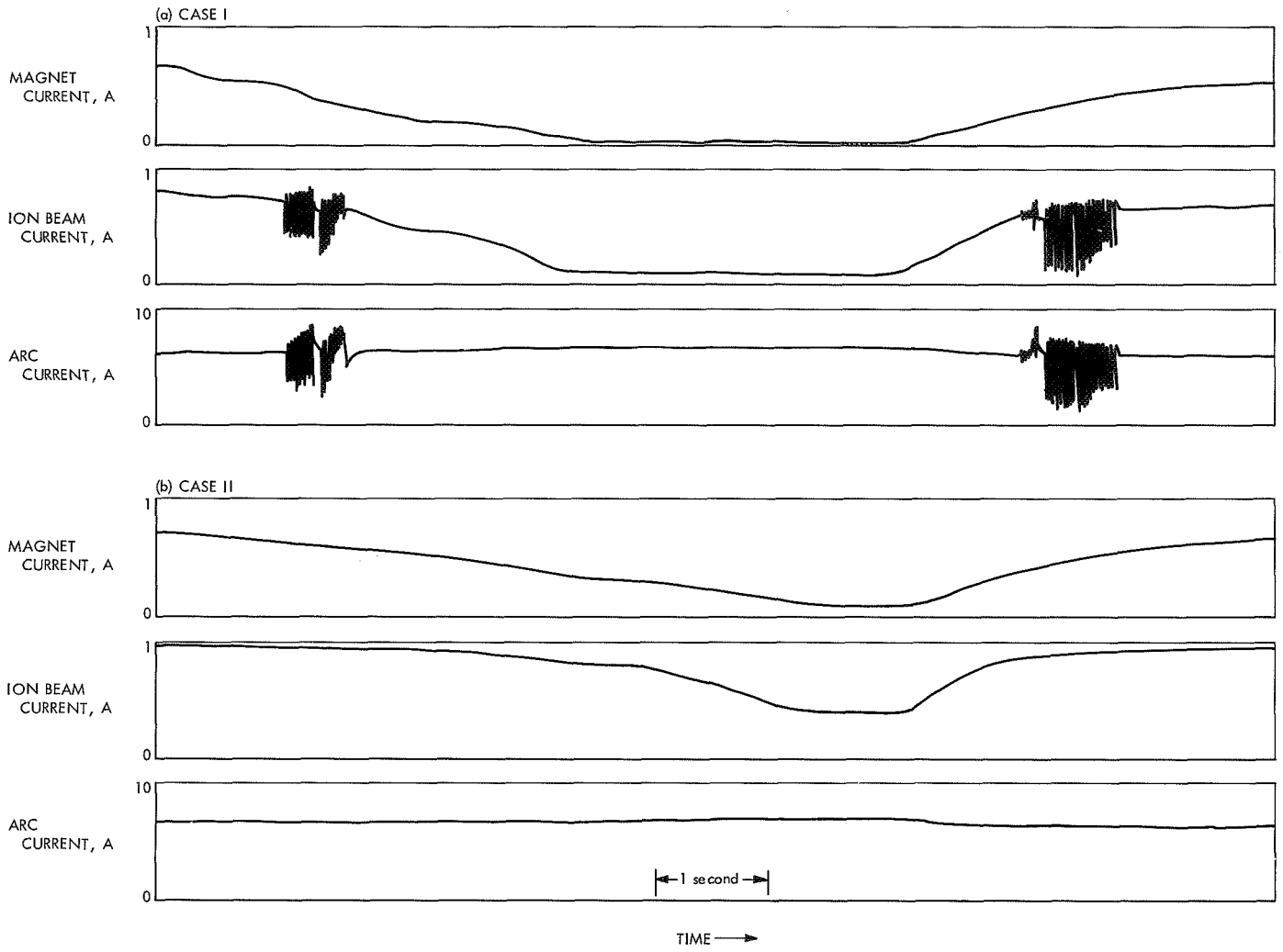

Fig. 4. Thruster response to variations in current to the electromagnets: (a) Case I, cathode mounted within pole piece; (b) Case II, keeper–baffle combination

oscillations that have been observed at low values of the thruster magnetic field. Typical thruster operation for variations in the current for the electromagnets is shown in Fig. 4 for both cases. The absence of the oscillations for the combination keeper–baffle geometry (Case II) should result in more stable thruster operation under conditions where a reduction in magnetic field is desirable, such as during automatic operation with a power conditioning unit (Ref. 1). This unit provides the controls and proper voltages to a thruster operating from a solar array. Reduction of the magnetic field provides a convenient way to restore thruster operation after a momentary shutdown to protect the power conditioner from arcing between the grids of the ion-accelerating geometry.

Operation with the combination baffle appeared to be more insensitive to the level of current drawn to the keeper. No regions of thruster operation were observed where it was necessary to draw high levels of keeper current in order to maintain the arc chamber discharge.

References

1. Pawlik, E. V., Costogue, E. N., and Schaefer, W. C., "Operation of a Lightweight Power Conditioner with a Hollow Cathode Ion Thruster," AIAA Paper 70-648, presented at the 6th Propulsion Joint Specialist Conference, San Diego, Calif., June 1970.

2. Bechtel, R. T., "Performance and Control of a 30-Centimeter Diameter Low Impulse Kaufman Thruster," AIAA Paper 69-238, presented at the 7th Electric Propulsion Conference, Williamsburg, Va., Mar. 1969.

3. King, H. J., and Poeschel, R. L., *Low Specific Impulse Ion Engine*, Final Report, NASA CR-72677. Hughes Research Laboratories, Malibu, Calif., 1970.

4. *Research on Hollow Cathodes in Mercury Ion Thrusters*, Final Report. Colorado State University, Fort Collins, Colo., Sept. 1970.

C. Thrust Subsystem Design for Nuclear Electric Spacecraft, *T. D. Masek*

1. Introduction

Nuclear-powered, electrically propelled, unmanned spacecraft are of interest for the 1980s (Ref. 1). The purpose of this study is to provide a method for estimating the mass and dimensions of the thrust subsystem for such a nuclear electric vehicle. A Jupiter orbiter was chosen as a reference mission. A 13,600-kg spacecraft, launched to a 700-nmi orbit by a *Titan* booster, spirals to escape velocity. A similar spiral maneuver is performed to obtain the Jupiter orbit. Mission duration is approximately 2 yr with 12,000 h of full-power operation at 240 kW into the thruster array. The general guidelines used in determining thrust subsystem size are as follows:

Total conditioned power to thrusters	240 kW
True specific impulse	5000 s
Thruster redundancy	20%
Attitude control	Electric propulsion system
Maximum envelope diameter	3.05 m
Thrust duration	12,000 h
Technology	Estimated for 1980

A design based on these parameters is shown in Fig. 1. The major features are illustrated in the drawing. The principle source of design information was Ref. 2.

2. Thruster

A typical thruster is shown schematically in the system drawing. This is a mercury bombardment-type thruster and is similar to that described in Refs. 3 and 4. Mercury was chosen over other propellants because of the present relatively well-developed technology of mercury systems.

Calculations, based on the present SE-20C thruster design (SPS 37-51, Vol. III, pp. 124–128), result in the following equation for thruster mass:

$$m_t = 1.85 + 57D_b^2 \tag{1}$$

where

m_t = individual thruster mass, kg

D_b = ion beam diameter, m

If the maximum current density of the SE-20C is assumed (32 A/m^2), the beam diameter in meters is given by

$$D_b = \frac{6.30 \times 10^2}{I_{sp}} (\eta_m \eta_t p_t)^{1/2} \tag{2}$$

where

p_t = individual thruster input power, kW

I_{sp} = true specific impulse, s

η_m = propellant utilization efficiency

$\eta_t = \eta_m \eta_p$ = total thruster efficiency

η_p = power efficiency

Combining Eqs. (1) and (2), we find

$$m_t = 1.85 + 2.26 \times 10^7 \frac{\eta_m \eta_t p_t}{I_{sp}^2} \tag{3}$$

The choice of the number of thrusters for a constant power system is mainly a trade-off of reliability (spares) against complexity (switching), and logic and total thruster mass. A convenient number of thrusters for this power level is 37. This provides reasonable packaging and six spares. Considering Ref. 5, this number of spares seems appropriate although reliability calculations were not made here. Considering switching and power conditioning requirements (and the associated complexity), this number of spares would provide a spare thruster for groups of four or five operating thrusters. Switching, logic, and spare power conditioning (PC) units could also be grouped in this way to reduce the extremely large number of possible thruster–PC combinations. Such a grouping scheme would make each group about the size and complexity of the JPL SEPST[1] III system (Ref. 6).

With 31 equal size operating thrusters, the input power per thruster is 7.75 kW. Using typical values of efficiency of $\eta_m = 0.90$ and $\eta_p = 0.92$ ($\eta_t = 0.83$ projected from Ref. 3 at a specific impulse of 5000 s), the thruster beam diameter is about 0.31 m and the mass per thruster is approximately 7.1 kg. These values were used in the present design.

The total thruster mass and the dependence of mass on the number of thrusters (for a given power) is of interest. In general, several thruster sizes could be used in a system. In such a case, the total thruster mass is

$$M_t = \sum_i m_{t,i} n_{t,i} \tag{4}$$

[1]SEPST = Solar Electric Propulsion System Technology.

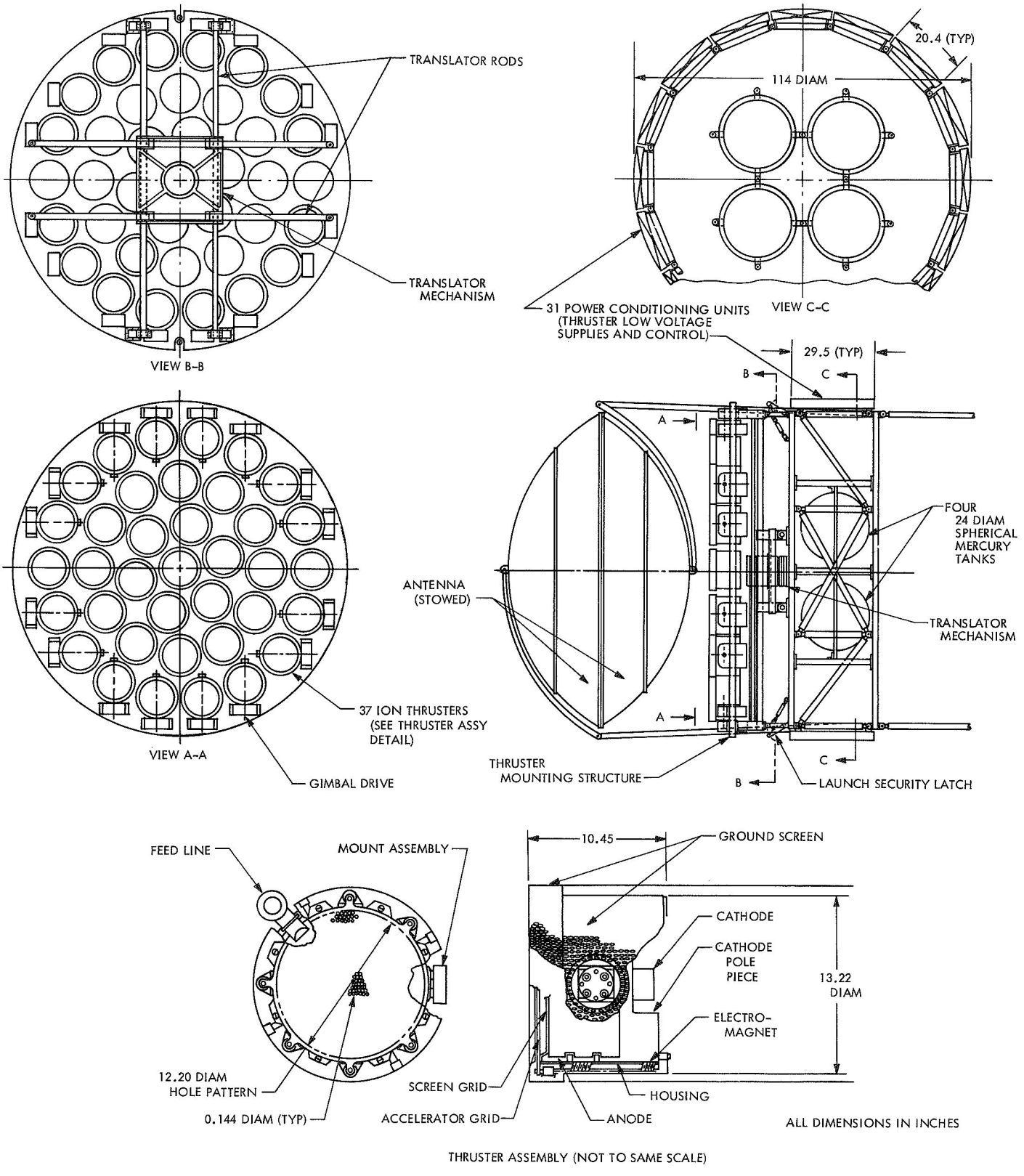

Fig. 1. 240-kWe nuclear-powered electric propulsion system

where $m_{t,i}$ is the mass of the ith thruster and $n_{t,i}$ is the number of ith thrusters. The total number of thrusters is given by

$$N_t = n_t + n_s$$

where

n_t = number of initially operating thrusters

n_s = number of initial spare thrusters

Similarly, the total thruster power is

$$P_t = \sum_i p_{t,i}\, n_{t,i} \tag{5}$$

where $p_{t,i}$ is the power level of the ith thruster. Using Eqs. (3) and (5), the total mass is given by

$$M_t = 1.85\,(n_t + n_s) + 2.26 \times 10^{7}\,\frac{\eta_m \eta_t}{I_{sp}^2}\left(P_t + \sum_i p_{t,i}\, n_{s,i}\right) \tag{6}$$

If all thrusters are the same size, Eq. (6) becomes

$$M_t = 1.85\,(n_t + n_s) + 2.26 \times 10^{7}\,\frac{\eta_m \eta_t P_t}{I_{sp}^2}\left(1 + \frac{n_s}{n_t}\right)$$

or

$$M_t = \left(1.85 n_t + 2.26 \times 10^{7}\,\frac{\eta_m \eta_t P_t}{I_{sp}^2}\right)\left(1 + \frac{n_s}{n_t}\right) \tag{7}$$

For a fixed percentage redundancy, i.e., a constant value of $1 + (n_s/n_t)$, the trade-off of system weight versus thruster number is 1.85 kg per operating thruster. In the present case (with $\eta_m = 0.9$ and $\eta_t = 0.83$), the total mass is about 266 kg. A change in n_t of ⅓ ($\Delta n_t = 10$) results in a change in M_t of about 8%. Thus, the total thruster mass is not too sensitive to the choice of n_t.

As a first choice, equal size thrusters were chosen. This simplifies thruster and PC development. However, if the system detail design showed advantages in packaging or reliability with multiple sizes, the mass trade-off is small. In addition, the grouping scheme mentioned previously would minimize the effect of the reduced interchangeability with multiple sizes.

The beam voltage is determined by specific impulse and propellant utilization and is given approximately by

$$V_b = 10^{-4}\,\frac{I_{sp}^2}{\eta_m} \tag{8}$$

For $I_{sp} = 5000$ s and $\eta_m = 0.9$, $V_b = 3090$ V, and $\eta_p = 0.92$. Hence, for the 7.75-kW thruster, the beam current is about 2.3 A. This corresponds to a propellant flowrate of about 5.33×10^{-4} g/s.

3. Power Conditioning

Typical PC units are shown in Fig. 1. These were sized assuming 90% thruster power efficiency and that the units shown provide only the low power supplies and thruster controls. The beam power is assumed to be provided by a PC unit near the reactor. The area of the PC units shown assumes a panel temperature of 25°C and a conversion efficiency of about 90% (Ref. 5).

As an estimate of the PC mass, the specific mass is taken as 3.0 kg/kW of input (0.775 kW at 250 Vdc) power (Ref. 5). Thus, the mass per PC unit is about 2.3 kg.

4. Thrust Vector Control

A typical thrust vector control (TVC) design is illustrated in Fig. 1. This design provides three-axis attitude control (two-axis translation, one-axis gimbal). Calculations were not made to determine the needed translation distances or gimballing angles. Such calculations depend upon the spacecraft design. Thus, the weight and size of the mechanical portion of the TVC depend on the complete design.

As a first approximation, the TVC system shown in the system drawing was chosen. This design was based mainly on the 3.05-m envelope constraint. Assuming a translator actuator size, the translation distance is fixed. In this case, the translation distance along the translation axis is about 0.76 m.

An alternate approach to attitude control may be through the use of differential thruster throttling combined with gimballing. The large number of operating thrusters could possibly provide adequate control. However, multiple-axis coupling might require a substantial amount of logic for choosing the correct thrusters for throttling. Study would be needed to assess feasibility.

5. Switching Matrix

Switches are estimated to weigh about 2.7 kg per PC unit assuming six to eight-position switches are used. Such switches are consistent with the grouping scheme discussed previously. Thus, with 37 PC units, the switch weight would be about 220 lb. The switching logic is estimated to be about 13.6 kg. Each switch can be expected to be 3 or 4 in. in diameter and about 6 in. long.

6. Propellant Storage and Distribution

An estimate for the size of this element can be obtained by assuming the mass to be a fraction of the propellant mass. The total propellant flowrate during operation, defined in unconventional but more useful dimensions of kg/h, is

$$\dot{M}_p = \frac{0.75 \times 10^{-2} I_b}{\eta_m} = \frac{0.75 \times 10^{-2} \eta_p P_t}{\eta_m V_b}$$

or

$$\dot{M}_p = \frac{7.5 \times 10^4 \eta_c P_t}{I_{sp}^2} \tag{9}$$

where

I_b = total beam current, A

V_b = net beam voltage, kV

The total propellant used is

$$M_p = 7.5 \times 10^4 \int_{t_i}^{t_f} \frac{\eta_t P_t}{I_{sp}^2} dt \tag{10}$$

where t_i and t_f are propulsion start and finish times, respectively. If we now relate M_p to the propellant storage and distribution (PSD) mass M_{ps} by

$$M_{ps} = \gamma M_p$$

we find

$$M_{ps} = 7.5 \times 10^4 \gamma \int_{t_i}^{t_f} \frac{\eta_t}{I_{sp}^2} P_t \, dt \tag{11}$$

The factor γ (approximately 0.03) includes tankage, valves, feed lines, and miscellaneous fittings. Assuming that η_t, P_t, and I_{sp} do not vary with time,

$$M_p = 7.5 \times 10^4 \frac{n_t P_t}{I_{sp}^2} \Delta t \tag{12}$$

For a 12,000-h mission, $M_p = 7200$ kg. With a 10% contingency for operation off the desired utilization efficiency, the total propellant mass would be approximately 7920 kg. Using this, the PSD mass is about 240 kg.

The element masses are summarized in Table 1. Within the accuracy of the present estimates, a specific mass of 4 kg/kW appears to be reasonable.

Table 1. Element mass summary

Element	Unit mass, kg	Total, kg
Thruster (37) (including neutralizer)	7.1	263
Power conditioning (31)	2.3	71
Thrust vector control:		
Gimbals (16)	1.4	22
Translator	23.0	23
Structure	180.0	180
Electronics	23.0	23
Switching:		
Switches (31)	2.7	84
Electronics	13.6	13.6
Propellant storage and distribution	240.0	240
Miscellaneous (wiring, launch caging, adapters, etc.)	50.0	50
		969.6

References

1. Mondt, J. F., and Prickett, W. Z., "External-Fuel and Flashlight Thermionic Reactor Potential for Electric Propulsion," AIAA Paper 70-644, presented at the 6th Propulsion Joint Specialist Conference, San Diego, Calif., June 1970.

2. Masek, T. D., "Sizing a Solar Electric Thrust Subsystem," Technical Report 32-1504. Jet Propulsion Laboratory, Pasadena, Calif., Nov. 15, 1970.

3. Masek, T. D., and Pawlik, E. V., "Thrust System Technology for Solar Electric Propulsion," AIAA Paper 68-541, presented at the 4th Propulsion Joint Specialist Conference, Cleveland, Ohio, June 1968.

4. Masek, T. D., and Womack, J. R., "Experimental Studies with a Mercury Bombardment Ion Engine System," AIAA Paper 67-698, presented at the AIAA Electric Propulsion and Plasma Dynamics Conference, Colorado Springs, Colo., Sept. 1967. Also available as Technical Report 32-1280, Jet Propulsion Laboratory, Pasadena, Calif., July 15, 1968.

5. *Solar Powered Electric Propulsion Spacecraft Study*, Final Report SSD-50094-R. Hughes Aircraft Company, Culver City, Calif., Dec. 1965.

6. Masek, T. D., and Macie, T. W., "Solar Electric Propulsion System Technology," AIAA Paper 70-1153, presented at the 8th Electric Propulsion Conference, Stanford, Calif., Aug. 1970.

D. Ion Thruster Connectors, *E. T. Hopper*

1. Introduction

Solar electric propulsion system tests are now being conducted (Refs. 1 and 2) that involve integration of a power conditioner with an ion thruster. A small but important component in the system that has been of concern in flight tests (Ref. 3) is the single cable connector used to transfer power to the thruster. In the use of commercially available connectors, it was found that arcing occurred between disconnect pins and leads due to proximity of high-potential and low-potential lines. This resulted in the breakdown of components and of the systems life tests.

Arcing also occurred when high-pressure areas developed in the connector due to poor pump-out conditions or out-gassing of components under normal operational testing.

Failures experienced while using a conventional disconnect prompted development of a design using an approach similar to that used in Ref. 4. Successful operation has been accomplished with no breakdowns over more than 200 h of operation.

2. Apparatus

The connector was used during the normal integration tests of a 20-cm thruster (Fig. 1) with a power conditioner system. Table 1 shows the voltages and grouping involved. The connector selected (MS 3102A-28-21P) was a standard production type, modified as follows:

(1) All aluminum parts were chemically stripped of zinc chromate, cadmium, and copper.

(2) The plastic insulator parts were removed and replaced with boron nitride (Fig. 2).

Table 1. Voltage and groups

Voltage	Group
High voltage (+2000 V)	Magnet Anode Cathode vaporizer Cathode vaporizer thermocouple Cathode keeper Cathode heater Common
Low voltage (ground potential voltage)	Main vaporizer Main vaporizer thermocouple Neutralizer vaporizer Neutralizer cathode Neutralizer keeper Neutralizer common Neutralizer vaporizer thermocouple
Accelerator high voltage (−1000 V)	Accelerator grid

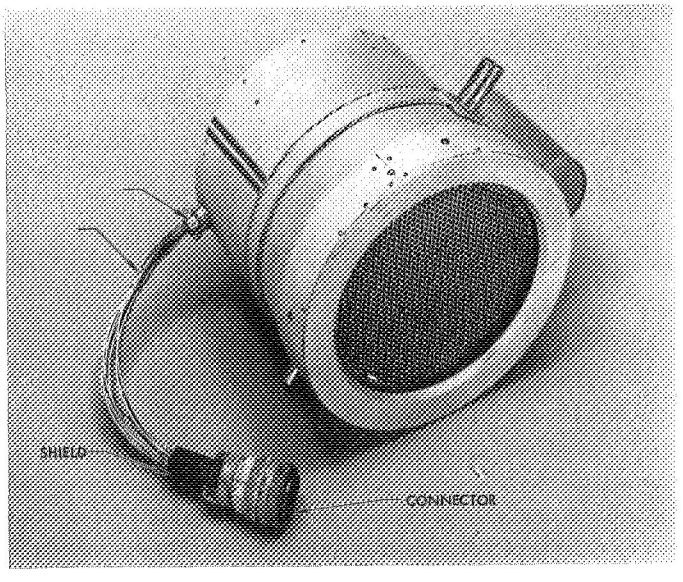

Fig. 1. 20-cm-diam ion thruster and cable connector

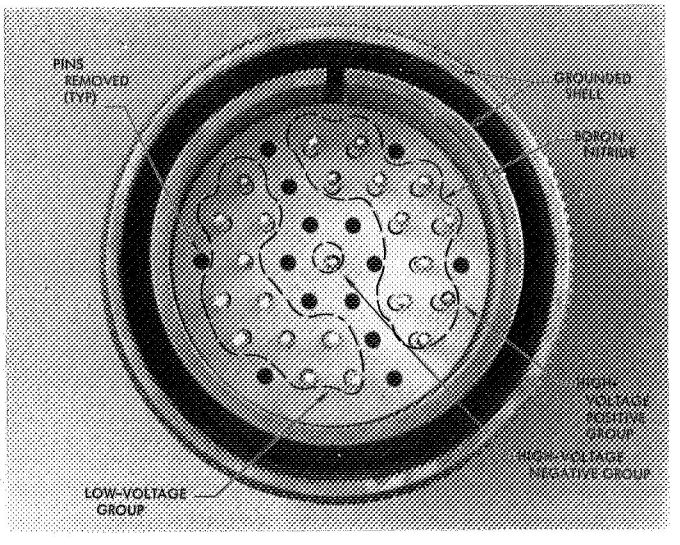

Fig. 2. Internal view of connector, showing various voltage groups

(3) Connector pins (Fig. 2) were removed in a pattern so as to leave the remaining pins in three separated groups, each group having a different potential. The removal of pins allowed a free pump-out path in all areas of the connector to avoid local high pressures. The removal pattern also allowed much longer creepage paths between different potential groups.

In addition, special precautions were instituted to minimize interwire breakdowns in the cable. Power and thermocouple leads both have Kapton Conformal-wrapped insulation. All leads were also sheathed with Teflon sleeving at the thruster feedthrough clamp, while, at the connector, the conventional plastic insulator sleeve was used as a shadow shield against back sputtered vacuum tank material and left unclamped to facilitate faster pump-out.

Connector pins were silver-soldered into the pins and all flux removed. All sharp edges and points were then smoothed to large radii.

3. Test Results

The connector was bench checked to an applied voltage of 5 kV between voltage groups at ambient temperature and atmospheric pressure. Less than 0.1 μA leakage was noted in this test. The connector was then installed in the thruster system with the connector body electrically grounded. The portion of the thruster system located within the vacuum tank (i.e., feedthroughs, thruster connector, thruster, insulators, wiring) was high-voltage checked at atmospheric conditions prior to installation within the vacuum chamber. At 3.5 kV, less than 0.5 μA leakage existed within this system.

The thruster was operated in 10- to 20-h intervals as part of a test program involving internal thruster geometry changes. At the end of each test interval the connector was examined and the system was retested as part of the normal thruster checkout procedure. No appreciable deposits of metal were noted at the rear of the connector when the protective shadow shield was removed. Thruster checkout including cable and connector was performed after each test operation of the thruster system and the cable and connectors were examined for breakdowns. No damage to the insulation was observed. The creepage paths between voltage groups were free from contamination and arc trails. High-voltage checking of the system showed no deviation from the original test setup.

4. Conclusions

The connector tests indicate its applicability for use in a systems life test of 1000 to 10,000 h.

The same configuration could possibly be considered for flight applications if Al_2O_3 were used in place of boron nitride as the insulator material and stainless steel in place of the aluminum shell. Such a part is commercially available.

References

1. Masek, T. D., and Macie, T., *Solar Electric Propulsion System Technology*, AIAA Paper 70-1158, presented at the 8th Electric Propulsion Conference, Stanford, Calif., Aug. 1970.
2. Pawlik, E. G., Costogue, E. N., and Schaefer, W. C., *Operation of a Lightweight Power Conditioner With a Hollow Cathode Ion Thruster*, AIAA Paper 70-648, presented at the AIAA 6th Propulsion Joint Specialist Conference, June 1970.
3. Rulis, R. J., *Design Considerations and Requirements for Integrating an Electric Propulsion System Into the SERT II and Future Spacecraft*, AIAA Paper presented at the 8th Electric Propulsion Conference, Stanford, Calif., Aug. 1970.
4. Paul, F. W., and Burrow Bridge, D., "The Prevention of Electrical Breakdown in Spacecraft," NASA SP-208, Goddard Space Flight Center, Greenbelt, Md., 1969.